



Cite this: *Analyst*, 2023, **148**, 5926

Quantitative detection of RAS and KKS peptides in COVID-19 patient serum by stable isotope dimethyl labeling LC-MS†

Ben K. Ahiadu,^a Thomas Ellis,^a Adam Graichen,^a Richard B. Kremer^b and James F. Rusling^{id} ^{*a,c,d,e}

Angiotensin and kinin metabolic pathways are reported to be altered by many diseases, including COVID-19. Monitoring levels of these peptide metabolites is important for understanding mechanisms of disease processes. In this paper, we report dimethyl labeling of amines in peptides by addition of formaldehyde to samples and deuterio-formaldehyde to internal standards to generate nearly identical isotopic standards with 4 *m/z* units larger per amine group than the corresponding analyte. We apply this approach to rapid, multiplexed, absolute LC-MS/MS quantitation of renin angiotensin system (RAS) and kallikrein-kinin system (KKS) peptides in human blood serum. Limits of detection (LODs) were obtained in the low pg mL⁻¹ range with 3 orders of magnitude dynamic ranges, appropriate for determinations of normal and elevated levels of the target peptides in blood serum and plasma. Accuracy is within ±15% at concentrations above the limit of quantitation, as validated by spike-recovery in serum samples. Applicability was demonstrated by measuring RAS and KKS peptides in serum from COVID-19 patients, but is extendable to any class of peptides or other small molecules bearing reactive –NH₂ groups.

Received 9th June 2023,
 Accepted 6th October 2023
 DOI: 10.1039/d3an00943b
rsc.li/analyst

Introduction

Endogenous peptides regulate many human biological processes, including blood pressure, fluid, and electrolyte balance, and immune responses to foreign stimuli. Dysregulation of these peptides can cause undesirable biological effects, and these molecules can in principle be monitored to serve as biomarkers and reveal mechanisms underlying pathological conditions. While Immunoassays are valuable for detecting biomolecules, for small peptides they are often saddled with multiplexing, sensitivity, and selectivity issues^{1,2} although progress is being made in overcoming these limitations.^{3–5}

Liquid chromatography-mass spectrometry (LC-MS) offers high selectivity, easy multiplexing, and rapid assay development for multiplexed detection of peptides in biological samples.⁶ Quantitative LC-MS is often done using stable isotope dilution to account for variations in analyte recovery, ionization and/or detection. In the standard approach, a known amount of isotopically labeled standard is spiked into the sample at the earliest possible stage of preparation.^{7,8} While this approach offers high accuracy and selectivity in LC-MS quantitation of peptides, disadvantages include cost, time, and complexity of chemically synthesizing isotopically labeled standards for each analyte in a mixture.

Peptides can also be labeled using isobaric tags for relative and absolute quantitation (*i*TRAQ), isotope-coded affinity tags (*i*CAT), and tandem mass tags (*TMT*).⁹ Reductive amination has gained recent attention for fast, easy, low-cost isotopic labeling of peptides on amino groups enabling accurate, sensitive, selective, fast, multiplexed detection of proteins in comparative LC-MS proteomics.¹⁰ This method, often called stable isotope labeling (SIL), employs methylation of peptide amines using formaldehyde and subsequent reduction as first reported by Hsu *et al.*¹⁰ for comparative proteomic analyses of proteins in cell lysates.

We report here the application of SIL for absolute quantification of endogenous renin angiotensin system (RAS) and kallikrein-kinin system (KKS) peptide metabolites in serum from

^aDepartment of Chemistry, University of Connecticut, Storrs, Connecticut 06269, USA. E-mail: rusling.james@uconn.edu

^bDepartment of Medicine, McGill University Health Centre, 1001 Decarie Blvd., Montreal, QC H4A, Canada

^cDepartment of Surgery and Neag Cancer Center, UConn Health, Farmington, Connecticut 06232, USA

^dSchool of Chemistry, National University of Ireland Galway, Galway, H91 TK33, Ireland

^eInstitute of Materials Science, University of Connecticut, 97 N. Eagleville Road, Storrs, CT 06269, USA

†Electronic supplementary information (ESI) available. See DOI: <https://doi.org/10.1039/d3an00943b>

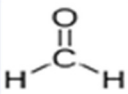
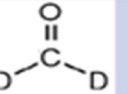


COVID-19 patients. Low-cost isotopic formaldehydes are used to differentially label multiple analyte peptides and standards that are mixed and analyzed in a single LC-MS/MS run. Deutero-formaldehyde and “light” formaldehyde react with primary and/or secondary amino groups in peptides to form Schiff’s bases and are then reduced by sodium cyanoborohydride to add methyl groups on each reactive amino moiety (Scheme 1). Unmodified primary amino moieties on N-termini and lysine residues of peptides are dimethylated by this reaction, while N-terminal proline residues are mono-methylated. Formaldehyde addition followed by sodium cyanoborohydride reduction converts free amino groups on analytes to dimethyl amines to produce a mass shift of 28 Da. Deutero-formaldehyde is added to standards followed by reduction to introduce a 32 Da mass shift. Thus, high-resolution accurate mass (HRAM) spectrometers enable selective detection of the deuterated standards and undeuterated sample species that differ in m/z but have very similar LC retention times.¹¹ Since first reported in 2003,¹⁰ stable isotope labeling by reductive amination has been further optimized¹² and widely used for relative quantitation of peptides from protein digestion in proteomics.^{13,14} Triple-quadrupole mass spectrometry in selected reaction monitoring (SRM) mode (or multiple reaction monitoring, MRM) is often used for LC-MS/MS quantification of peptides.¹⁵ However, identifying and constructing tran-

sitions for MRM can be labor-intensive. Parallel reaction monitoring (PRM) with high resolution accurate MS such as quadrupole-time of flight (Q-TOF) or quadrupole-Orbitrap spectrometers¹⁶ has primarily been utilized for targeted protein quantification *via* fragments of chosen surrogate peptide precursor ions. MRM and PRM have comparable sensitivity, precision, and linear dynamic range,^{17,18} but PRM has better selectivity, and enables faster method development.

In this paper, we describe stable isotope dimethyl-amination for quantitative PRM LC-MS determination of endogenous renin angiotensin system (RAS) and kallikrein-kinin system (KKS) peptide metabolites whose levels are reportedly altered in patients with COVID-19 and other diseases.^{19–22}

RAS and KKS metabolites play regulatory roles in humans (Scheme 2). RAS is a major regulator of blood pressure, fluid, and electrolyte balance^{23,24} while KKS controls vascular permeability, vasodilation, release of inflammatory cytokines during tissue injury, and cell proliferation.^{19,25} As discussed above, we utilize *in situ* SIL of amines with formaldehyde and internal standards with deutero-formaldehyde with cyanoborohydride reduction to generate isotopic standards differing in mass by +4 Da per reacted primary amine compared to sample peptides (Scheme 1). We demonstrate herein a wide linear dynamic range and limits of detection (LOD) in the low pg mL⁻¹ range for this new SIL peptide assay that was validated according to US Food and Drug Administration guidelines.²⁶ Applicability was demonstrated by measuring RAS and KKS metabolites in serum of COVID-19 patients.

	Light	Mid
Formaldehyde Isotope		
Cyanoborohydride Isotope	NaBH ₃ CN	NaBH ₃ CN
$\Delta M/1^\circ$ Amine	+ 28.0313	+ 32.0564

Scheme 1 Dimethyl labeling of amines in peptides. Light formaldehyde labeling is used for analytes; Mid or deutero-formaldehyde labeling is used for internal standards.

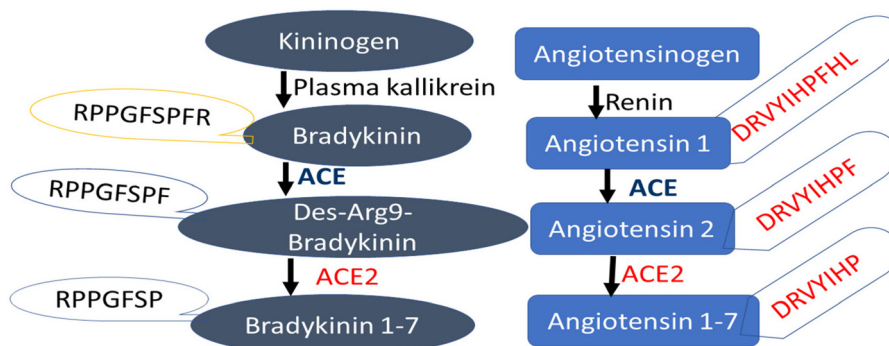
Experimental

Peptides and reagents

See ESI† for details about source of chemicals and reagents. Sample preparation and analysis procedures are further elaborated in the ESI.†

Stock solutions

To inhibit adsorption of peptides on reaction and storage vials, and enhance solubility, 1 mg mL⁻¹ stock solutions of individual peptides were made in 25% acetonitrile containing



Scheme 2 Kinin (left) and angiotensin peptide metabolic pathways that utilize enzymes angiotensin converting enzyme (ACE) and ACE2.



1% formic acid and stored at $-80\text{ }^{\circ}\text{C}$ until use. Appropriate volumes of each peptide stock solutions were mixed so that each analyte was $5\text{ }\mu\text{g mL}^{-1}$ in 0.1 M sodium acetate buffer, pH 5.5. Calibration standards were made from this working solution in pH 5.5 buffer containing 10% acetonitrile and stored in $90\text{ }\mu\text{L}$ aliquots at $-20\text{ }^{\circ}\text{C}$ for subsequent labeling. Similarly, quality control (QC) samples were made from a separate $5\text{ }\mu\text{g mL}^{-1}$ combined stock solution and stored at $-20\text{ }^{\circ}\text{C}$ until use. External standards and QC samples were spiked with $10\text{ }\mu\text{L}$ of 0.2% human serum to mimic the sample matrix. Pipette tips were pre-rinsed $3\times$ with respective solutions to saturate binding sites before solutions were transferred.

Internal standards

A deuterio-formaldehyde-labeled version of each analyte served as internal standard for quantifying formaldehyde-labeled endogenous metabolites. Internal standards were generated by reacting $8\text{ }\mu\text{L}$ of 4% (v/v) deuterio-formaldehyde with $100\text{ }\mu\text{L}$ of 5 ng mL^{-1} peptide standard for 3 min followed by reduction with $8\text{ }\mu\text{L}$ of 0.6 M sodium cyanoborohydride for 1.5 h. LC-MS analyses confirmed that reactions (Scheme 1) are complete (see Results).

Methylated internal standards were spiked into calibration standards, quality control (QC), and real samples at 300 pg mL^{-1} final concentration. To derivatize the analyte peptides, $16\text{ }\mu\text{L}$ of 4% normal formaldehyde (v/v) was added, vortexed, and allowed to stand for 3 min. The mixture was then incubated with shaking for 1.5 h at ambient temperature after adding $16\text{ }\mu\text{L}$ 0.6 M sodium cyanoborohydride (not deuterated) as reducing agent. The reaction was quenched with $16\text{ }\mu\text{L}$ of 1% ammonium hydroxide (v/v), then acidified and further quenched with $90\text{ }\mu\text{L}$ 0.1% formic acid. Reaction products were then isolated with solid-phase extraction (SPE).

Safety note

Because of toxicities of formaldehyde, sodium cyanoborohydride, and hydrogen cyanide released as a result of quenching and acidification of the samples, all reaction and quenching steps were performed under a fume hood.

Analysis of serum

Serum from COVID-19 patients ($n = 80$) were collected at McGill University Health Centre Research Institute (MUHC-RI) with approval (#2021-6081) from the center's Ethics Board. Serum samples of $30\text{ }\mu\text{L}$ were analyzed in duplicate. Samples were subjected to dimethyl labeling with formaldehyde as described above, and the deuterium-labeled internal standard was spiked into the serum at 300 pg mL^{-1} final concentration.

Solid phase extraction (SPE)

Salts and other interfering substances were removed from standards and serum samples using SPE. The SPE cartridges used were in a 96-well filter plate format (Oasis® HLB μ Elution Plate $30\text{ }\mu\text{m}$, 186001828BA, Waters). Wells of the 96-well plate were conditioned using $200\text{ }\mu\text{L}$ methanol ($2\times$) followed by equilibration using $200\text{ }\mu\text{L}$ water ($2\times$). Samples acidi-

fied to pH 2.8 were then loaded into the wells and allowed to drain at 1 mL min^{-1} under vacuum, followed by washing with 0.1% formic acid in water ($12\times$) and a final wash with 5% acetonitrile in water containing 0.1% formic acid. Analytes were then eluted from the wells using $150\text{ }\mu\text{L}$ each of 30% acetonitrile, and 60% acetonitrile containing 0.1% formic acid. This effectively eluted hydrophilic and hydrophobic analytes. Eluates were then dried in a vacuum centrifuge at $60\text{ }^{\circ}\text{C}$ and reconstituted in $50\text{ }\mu\text{L}$ of 10% acetonitrile containing 0.1% formic acid.

Instrumentation and software

Liquid chromatography was done using a Thermo Fisher Scientific UPLC with temperature control at $45\text{ }^{\circ}\text{C}$. $25\text{ }\mu\text{L}$ of reconstituted sample or standard was injected and separated on a Phenomenex® Kinetex® $1.7\text{ }\mu\text{m}$ C18 $100\text{ }\text{\AA}$ LC column, $50\text{ mm} \times 2.1\text{ mm}$, fitted with a Phenomenex SecurityGuard Ultra C18 (AJ0-8782) precolumn. The autosampler was operated at $4\text{ }^{\circ}\text{C}$. Water containing 0.1% formic acid was used as mobile phase A, while mobile phase B contained acetonitrile with 0.1% formic acid. A 7 min binary gradient elution was used at a flow rate of $300\text{ }\mu\text{L min}^{-1}$, starting with a 6 min column equilibration step at 10% B prior to the gradient. Mobile phase B was then increased linearly to 24% until 7.3 min, to 95% until 7.4 min and kept at 95% to remove strongly retained impurities for 1.9 min before decreasing to 10% after 20 s.

The LC was coupled to an Orbitrap Exploris 480 mass spectrometer (Thermo) via a heated electrospray ionization (HESI) source (KQ Integrated Solutions, Inc.). The ionization source was operated in the positive ion mode at spray voltage of 4000 V, with sheath gas at 60 arbitrary units and auxiliary and sweep gases at 15 and 2 arbitrary units, respectively. Ion transfer tube temperature was $300\text{ }^{\circ}\text{C}$, while the vaporizer was at $400\text{ }^{\circ}\text{C}$. Thermo XCalibur software was used to control the system, while an open-source software Skyline (version 22.2.0.351) was used to analyze raw data. To verify proper peak detection and integration, every peak integrated was inspected manually.

Parallel reaction monitoring (PRM) was utilized for quantification, and a full scan was done to evaluate the efficacy of dimethyl labeling and to select the most intense, interference-free precursors for each peptide. The precursors and collision energies optimized for specific peptides are listed in ESI Table S1.† To ensure that all metabolites reacted fully, a full scan was done to confirm that the highest concentration standard in the calibration curves did not contain peaks for unreacted peptides.

A full scan (MS) was initially run on light and medium-labeled standards to identify the most intense precursor peaks and charge states. Precursors were subjected to fragmentation, and all fragment ions were monitored and recorded. Chromatogram traces of the fragment ions were then used to optimize the LC separation and ion source conditions. The MS/MS chromatograms were imported into Skyline to identify the retention time of each peptide. The retention times were



then exported back into the XCalibur method editor to create a retention time-scheduled parallel reaction monitoring (PRM) method (ESI Table S1†). Next, collision energies were optimized for each peptide by comparing the energy distribution and fragment ion intensities of each peptide at each tested normalized collision energy. A sum of at least three most intense co-eluting fragment peaks having zero background interference were used for quantifying each peptide. A peptide was deemed detected when (i) its light-labeled version co-elutes with the respective labeled internal standard; and (ii) the mass error of the representative fragments does not exceed 6 ppm.

Method validation

Validation was according to US Food and Drug Administration guidelines²⁶ in terms of linearity, accuracy, precision, recovery, sensitivity, carryover, and analyte stability.

Linearity, accuracy, precision (intra- and inter-day) and sensitivity. Accuracy, expressed as the relative error in the determined concentration of the quality control (QC), should be within $\pm 15\%$ of the nominal concentration of QCs significantly above the limit of detection (LOD) while a QC at or close to the LOD can have a relative error within 20% of the nominal QC concentration. Precision is a measure of the consistency of values obtained by the method and expressed as percent relative standard deviation of the mean concentration. The linearity of the method was evaluated using calibration curves constructed using linear regression in triplicate. We used QCs at four different concentrations (near the LOD, low, medium, and high concentration) in triplicate to assess accuracy and precision of the method. LOD was determined as $3\text{sd}/m$, and LOQ as $10\text{sd}/m$ where sd denotes standard deviation of replicate blank measurements and m is the slope of the calibration curve of the metabolite.

Carryover

This is a measure of the extent to which analytes from previous injections remain in the LC-MS (especially on the chromatographic column) and get detected in subsequent runs. Carryover was assessed by measuring analytes in a solvent blank after measuring the standard with highest concentration. A solvent blank was injected after the highest concentration standard was run alternately five times and the average peak areas of the analytes were computed.

Stability test

Stability of the samples was assessed at two handling conditions namely, the autosampler temperature and storage at -20°C . First, analytes were spiked into a 100% pooled human serum, labeled, and analyzed immediately. Then, they were stored in the autosampler at 4°C for three days. The samples were re-analyzed on the third day, and the peak areas on the first and third days were compared to determine the extent of analyte stability. Also, the stability of endogenous metabolites was assessed by spiking the metabolites into pooled human serum and storage at -20°C for 16 days. Signals were com-

pared to spiked samples that were freshly prepared and analyzed without storage.

Results

The SIL LC-MS peptide analysis method utilizing PRM was validated and applied to quantitatively determine key RAS and KKS metabolites. COVID-19 patient serum samples, calibration and internal standards were isotopically labeled using the dimethylation protocol (Scheme 1 and Fig. S1†). Calibration standards and COVID-19 samples were labeled using light-formaldehyde while internal standards were labeled with deuterio-formaldehyde. Optimized reaction conditions ensured that both formaldehyde- and D_2 -formaldehyde-labeled isoforms of each peptide were successfully generated. No peaks were found in full scan MS-detected chromatograms of any of the labeled peptides that would indicate side products or unreacted pep-

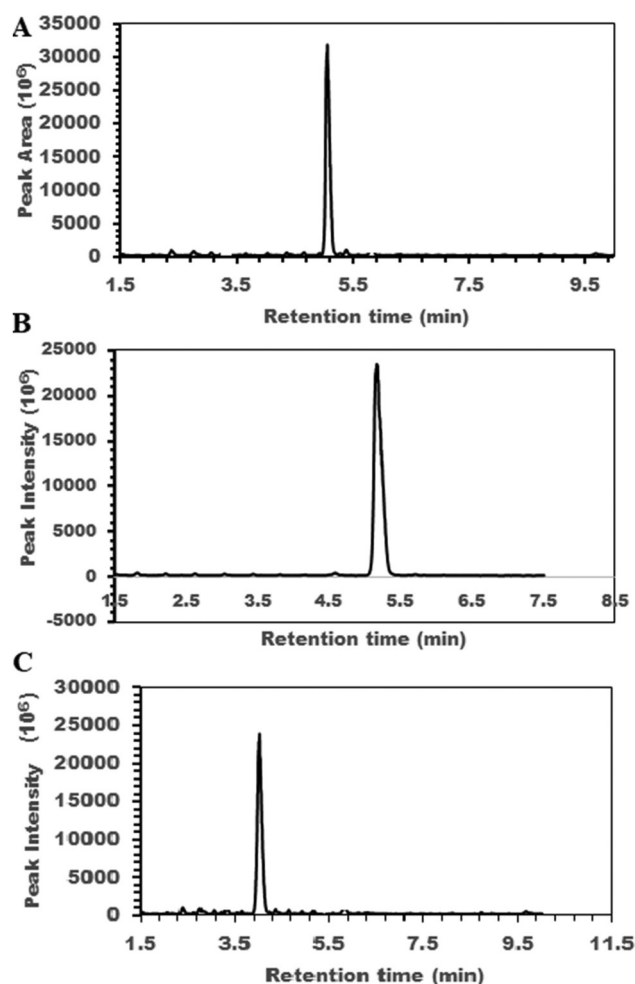


Fig. 1 LC chromatograms of 3 of the labeled peptides obtained using full MS1 scan, consistent with successful quantitative labeling of peptides with no side products. Chromatograms of (A) formaldehyde-reacted Brad; (B) formaldehyde-reacted des-R9-Brad; and (C) formaldehyde-reacted Brad 1–7. Also see ESI Fig. S2–S10.†



tides when the reducing agent was added immediately after 3 min reaction with formaldehyde, and reduction was done for 1.5 h (Fig. 1 and ESI Fig. S2, S3†). Labeling efficiency of $98 \pm 2\%$ was estimated by comparing full scan chromatograms and mass spectra of samples before and after labeling, as discussed below. Fig. 1 shows a single full MS scan chromatographic peak for each of 3 labeled peptides. A full scan chromatogram of the unlabeled complete peptide mixture showed seven major peaks (Fig. S2A†), representing the unlabeled peptides while a similar scan of the labeled sample also shows seven major peaks for formaldehyde-labeled peptides with similar retention times (Fig. S2B†). No other peaks were observed apart from the labeled peptide peaks. Fig. S3† shows similar full scan LCs of those labeled peptides not shown in Fig. 1. Fig. S4–S10† show mass spectra of each of the major peaks in the chromatogram with m/z ratios for the $z = 1, 2$ and 3 (in some cases) ions. m/z differences between D_2 -formaldehyde- and formaldehyde-labeled peptides are consistent with the differences in mass of the labels and indicate again that all starting peptides have been quantitatively labeled.

Optimized LC-MS provided sufficiently resolved chromatograms for all target metabolites (Fig. 2). Both light and medium labeled versions of each peptide had the same chromatographic retention times (inset in Fig. 2), a crucial requirement for precise and accurate quantitation.

Linearity, accuracy, precision (intra- and inter-day) and sensitivity

Calibration curves were constructed for each labeled metabolite (Fig. 3 and Fig. S11†) in 0.02% human serum to assess

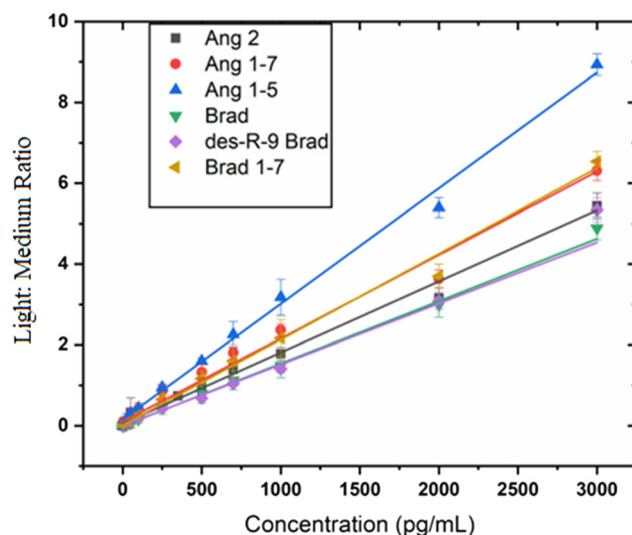


Fig. 3 Calibration curves using chromatographic peak area ratio of sample/deuterated standard showing linear response for each analyte. Analyte detection and quantitation was done using parallel reaction monitoring (PRM).

linearity. Best fits were estimated using linear regression with standard concentrations from low pg mL^{-1} to 3000 pg mL^{-1} for all analytes except Ang 1 whose upper range extends to 5000 pg mL^{-1} . Each analyte gave a linear plot with correlation coefficients $r > 0.99$. Lower limits of detection (LOD) ranging from 1.7 pg mL^{-1} to 67 pg mL^{-1} for all the different peptides (Table 1) were obtained.

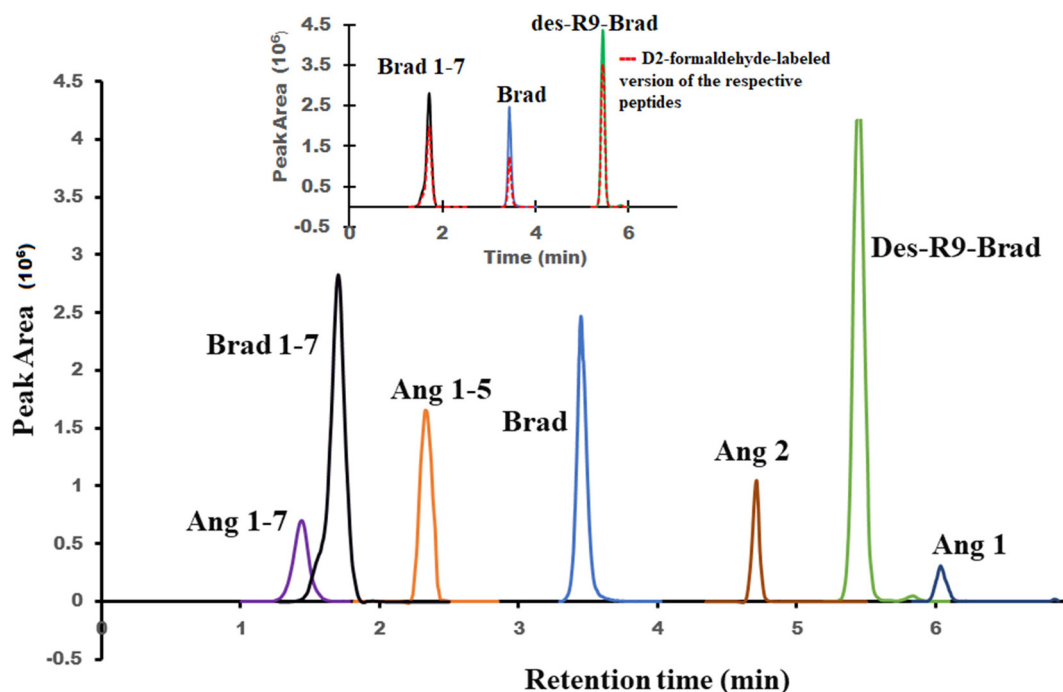


Fig. 2 Chromatographic elution profiles of peptide analytes. Both formaldehyde and D_2 -formaldehyde labeled versions of each analyte have nearly identical retention times (inset is an example of formaldehyde and D_2 -formaldehyde labeled kinins with approximately the same retention times) on the C18 column. Chromatograms were obtained using a full MS1 scan.



Table 1 Linear regression *r*-values and limits of detection (LOD) for each analyte

Peptide	Peptide sequence	<i>r</i> -Value	LOQ, pg mL ⁻¹
Ang 1	DRVYIHPFHL	0.9954	200.0
Ang 2	DRVYIHPF	0.9977	233.0
Ang 1–7	DRVYIHP	0.9981	44.0
Ang 1–5	DRVYI	0.9977	57.0
Brad	RPPGFSPFR	0.9959	40.0
Des-R9-Brad	RPPGFSPF	0.9976	5.3
Brad 1–7	RPPGFSP	0.9992	5.7

Spike-recovery studies

Intra- and inter-day accuracy and precision were estimated using pooled human serum spiked with three or four different concentrations of analyte, (depending on LOD of analyte) in triplicate. The intra-day accuracy and precision were within $\pm 20\%$ as stipulated for concentrations at the lower limit of quantitation (LLOQs), and $\pm 15\%$ for quality control samples (QCs) at all other concentrations. Accuracy and precision were $\leq \pm 15\%$, in compliance with the US FDA guidelines.²⁶ Individual accuracy and precision values are shown in ESI Table S2.† Solvent blanks run after the most concentrated external standard showed no signals for the analytes, indicating no carryover of analytes to successive runs.

Stability studies indicated that short-term storage of the native peptide samples at -20°C and labeled peptides at autosampler temperature of 4°C is appropriate. The stability in the autosampler was tested on labeled samples after extraction, and showed no effects of running long autosampler queues on the stability of the labeled analytes. Signal intensities of freshly prepared samples and those stored at -20°C for 16 days were almost identical (ESI Fig. S12†). Also, analyte signals remained stable (ESI Fig. S13 and S14†) during storage at the autosampler temperature of 4°C for at least three days.

COVID-19 samples

Serum samples from COVID-19 patients were analyzed, and averages for the analyte peptides were compared to averages obtained for 3 different batches of pooled human serum from healthy donors as surrogate controls. Age and sex matching of samples from surrogate healthy donors with those from COVID patients was not possible as the healthy samples were obtained from commercial sources. Results expressed in box and whisker plots indicate that RAS and KKS peptides in the 80 COVID-19 patients vary widely in concentration (Fig. 4). Indicated by low *p*-values except for Ang 1–7 (Table 2), average peptide concentrations in healthy controls differ significantly from values obtained in COVID-19 patients. All RAS peptides were downregulated in COVID-19 relative to the surrogate controls while the KKS counterparts were upregulated on average.

Discussion

SIL was successfully applied to LC-MS analyses of key RAS and KKS metabolites in COVID-19 patient serum (Fig. 4). LODs

were in the $1.6\text{--}13.2\text{ pg mL}^{-1}$ range for all but Ang1 and Ang2 which were 60 and 67 pg mL^{-1} (Table 1), respectively, sufficiently low to detect these peptides in normal patient blood serum. Accuracy and precision are better than $\pm 15\%$, at peptide levels above the limits of quantitation. Wide dynamic ranges obtained (Fig. 3) are also important for detecting varied levels of RAS and KKS metabolites in other biofluids.^{27,28} The method utilizes low-cost commercially available reagents to rapidly generate isotopic labels in serum samples and internal standards *in situ*, at a reagent cost of $\sim \$1$ per sample. This is the first assay to our knowledge designed for multiplexed endogenous peptide determinations by SIL-LC-MS in human biofluids. The method utilizes relatively small sample volumes and was successfully applied to an initial investigation of these two sister peptide metabolite systems in patients with COVID-19 infections (Fig. 4).

Side-reactions in formaldehyde-based SIL, with products described as *N*-methyl-4-imidazolidinone moieties, have been recently reported for reductive dimethylation of peptides using formaldehyde and sodium cyanoborohydride.²⁹ They form by slow intramolecular nucleophilic addition, and can influence accuracy and precision of subsequent quantitative LC-MS. We optimized SIL reaction conditions to enable complete dimethylation of each free amine in the peptides with no detectable side-products, intermediates, or unlabeled metabolites (Fig. 1, Fig. S2–S10†). Reducing agent added after the formaldehyde and briefly mixed with the sample blocks side-reaction pathways and enables rapid reduction of the Schiff's base. Excess amounts of reagents coupled with amine-free buffer ensure a complete, efficient reaction. We observed as reported previously²⁹ that reductive amination is pH sensitive and occurs at lower pHs without side-product formation. We thus utilized sodium acetate buffer pH 5.5 to provide optimum pH.

SIL forms of each peptide analyte and standard have nearly identical retention times, ensuring accurate and precise quantitation. This is attributable to three factors: (i) the small size of the SIL agent relative to the peptides, (ii) the relatively small number of deuterium atoms in each standard label, and (iii) the nearness of the deuterium isotopes to a hydrophilic site in the peptide.³⁰ Methyl groups bearing two or no deuterium atoms are too small to significantly influence the retention time of peptides with at least 5 amino acids. In addition, the peptides are derivatized at only one polar site which naturally has little hydrophobic interaction with the reversed-phase stationary phase. The fewer the labeling sites, the smaller the isotope effect on LC retention time.

Linear calibration curves were obtained with correlation coefficients greater than >0.99 for each analyte (Fig. 3). Internal standards were spiked into samples prior to labeling of the sample to minimize variations between samples, and loss of peptides. Once labeled with deuterio-formaldehyde, the internal standard was no longer reactive towards formaldehyde. Therefore, internal standard was spiked into the samples prior to their derivatization with formaldehyde. Preliminary results underscored the importance of this, as calibrations curves generated using internal standards spiked at latter stages of sample preparation were not linear.



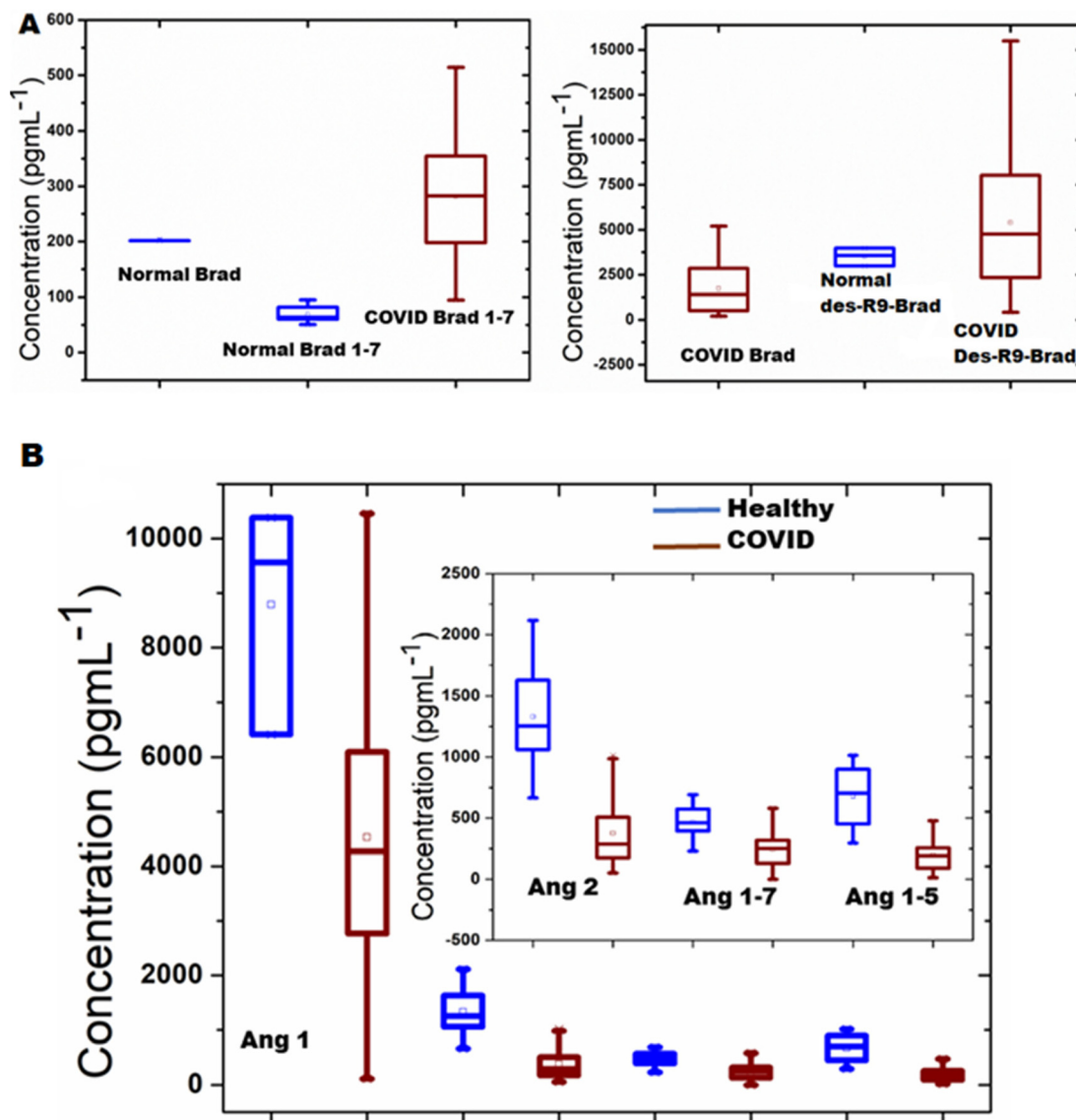


Fig. 4 Box and Whisker plots showing the distributions of mean peptide concentrations in non-COVID pooled human sera (blue) and serum from 80 COVID-19 patients (dark red). A. Normal and COVID-19 serum levels of KKS peptides. B. Normal and COVID-19 serum levels of RAS peptides.

Table 2 Averages of RAS-KKS peptides in COVID serum ($n = 80$) compared to concentrations in surrogate healthy controls ($n = 3$)

Analyte	Average \pm SD in healthy subjects (ng mL ⁻¹)	Average \pm SD in COVID patients (ng mL ⁻¹)	Fold change (%)	p -Value
Ang 1	8.8 (± 1.7)	4.50 (± 2.5)	-95.6	0.04
Ang 2	1.33 (± 0.3)	0.38 (± 0.2)	-71.7	0.03
Ang 1-7	0.47 (± 0.13)	0.24 (± 0.16)	-96.7	0.08
Ang 1-5	0.68 (± 0.12)	0.20 (± 0.28)	-71.2	0.01
Brad	0.20 (± 0.001)	1.73 (± 1.3)	756.4	<0.001
Brad 1-8	3.51 (± 0.5)	5.4 (± 1.9)	53.8	0.004
Brad 1-7	0.07 (± 0.02)	0.28 (± 0.1)	308.9	<0.001

The sensitivities of the new SIL method are comparable to sensitivities of a recently reported method to determine kinin peptides²⁷ but are far better than sensitivities reported for

other studies.^{28,31} Spike-recovery results were within the acceptable 85%–115% range except for Ang 2 at low level of 50 pg mL⁻¹ and Brad at 800 pg mL⁻¹. Carry-over in the LC was minimal, and analytes were stable for short-term storage at -20 °C and in the autosampler at 4 °C.

We found a decrease in average levels of all RAS peptides in serum from COVID-19 patients compared to levels in pooled human sera from healthy donors, while all KKS peptides in COVID-19 patients were upregulated from these controls. Thus, dysregulation of RAS and KKS peptides may play a role in the pathogenesis of COVID-19. Other studies have investigated RAS and KKS peptides separately.^{32–34} Our findings agreed with earlier downregulations reported for RAS peptides³² in COVID-19, though our values are higher than previously reported. Similar observations were made by Martins *et al.* but in their system, Ang 1 concentrations remained



unchanged while Ang 1–7 levels were elevated in plasma samples from critically ill COVID-19 patients.³⁵ The differences in analyte concentrations reported by different research groups may be due to such factors as the geographical origin of the samples and the specific strain of the SARS-CoV-2 virus, among others. However, serum levels of some RAS peptides were also reported to be unchanged in COVID patients^{33,34} and differ from other reports that suggested an upregulation of some of the RAS peptides and downregulation of others.^{36,37}

Our results show an increase in averages of all KKS peptides in COVID-19 patients relative to controls, which had not previously been reported for COVID-19. Bradykinin is known to induce vasodilation and vascular permeability.³⁹ Its increase in COVID-19 may be responsible for the difficulty in gas exchange experienced by critically ill patients as more fluids leak into their lungs than needed. The current results on the KKS agree with the observations made by Garvin *et al.*³⁸ about the upregulation of KKS components necessary to produce Bradykinin. Their study on fluids and cells from the lungs of COVID-19 patients observed an increase in kininogen and kallikreins that are required to produce Brad. Additionally, Garvin *et al.* reported that angiotensin converting enzyme (ACE) levels were lower in bronchoalveolar fluids (BALF) from COVID-19 patients. This decrease in ACE further explains our observed accumulation of Brad in serum samples from COVID-19 patients. It is also expected that the upsurge in Brad during SARS-CoV-2 infection would lead to the activation of the KKS receptors, especially the BDKRB2. Stimulation of this receptor leads to inflammation,³⁹ which further induces the release of des-R9-Brad and its receptor, BDKRB1.⁴⁰ The increased release of these two KKS receptors in the BALF of COVID-19 patients has been reported.³⁸ Furthermore, Garvin *et al.* reported that angiotensin converting enzyme 2 (ACE2) was over expressed in COVID, which may explain the elevated concentrations of Brad 1–7 we observed in the serum samples from COVID-19 patients.

It was recently reported that des-R9-Brad and Brad 1–7 levels in plasma and bronchoalveolar lavage fluids of COVID-19 patients were significantly higher, but with lower Brad levels compared to baseline concentrations.^{41–43} This slight difference in Brad regulation in the current and earlier studies is likely to be caused by the difference in the biofluids analyzed. While our preliminary analysis suggests that dysregulation of both RAS and KSS may be involved in pathogenesis of COVID-19, further data analyses related to disease severity, and studies of additional patient cohorts are needed before a definitive conclusion can be reached.

In summary, our results demonstrate an efficient SIL LC-MS method for quantitative, multiplexed analysis of RAS and KSS peptides at levels applicable to human serum. This cost-efficient strategy can be utilized for absolute quantitation without the common problems previously reported for dimethyl labeling and without laborious synthesis and purification of isotopic standards. This quantitative SIL method detects peptides in the low pg mL⁻¹ to high pg mL⁻¹ ranges with excellent precision and accuracy. Its use can contribute to

valuable future insights into metabolic alterations of peptide families that may occur in patients with different diseases, providing improved understanding of pathogenesis and biomarker guides for targeted therapies.

Author contributions

The project plan was conceived by Richard B. Kremer and James F. Rusling while Ben K. Ahiadu and Thomas Ellis developed the LC-MS/MS method with technical guidance and contributions from Adam Graichen. COVID data were collected and analyzed by Ben Ahiadu under the supervision of James F. Rusling. The manuscript was written by Ben Ahiadu and James Rusling while Richard B. Kremer contributed to the revisions of the text and supplied the COVID-19 patient samples.

Ethical statement

All experiments were performed in accordance with Canadian Guidelines stated in “regulatory framework in health research at the McGill University Health Center” and approved by the ethics committee of the “McGill University Health Center”. Informed consents were obtained from human participants of this study.

Conflicts of interest

The authors declare no conflict of interest.

Acknowledgements

The authors are grateful for funding from and the University of Connecticut Research Excellence Program and the Paul Krenicki Professorship. We thank Dr Catalin Mihalcioiu from the McGill UHC for providing access to his biorepository.

References

- 1 R. D. Grange, J. P. Thompson and D. G. Lambert, *Br. J. Anaesth.*, 2014, **112**(2), 213–216.
- 2 G. W. Boyd and W. S. Peart, in *Handbook of Experimental Pharmacology*, ed. I. H. Page and F. M. Bumpus, Springer, Berlin, Heidelberg, 1974, p. 37, DOI: [10.1007/978-3-642-65600-2_11](https://doi.org/10.1007/978-3-642-65600-2_11).
- 3 X. Wang, L. Cohen, J. Wang and D. R. Walt, *J. Am. Chem. Soc.*, 2018, **140**(51), 18132–18139.
- 4 Y. Li, G. Zhang, X. Mao, S. Yang, K. De Ruyck and Y. Wu, *TrAC, Trends Anal. Chem.*, 2018, **103**, 198–208.
- 5 P. Chen, M. T. Chung, W. McHugh, R. Nidetz, Y. Li, J. Fu, T. T. Cornell, T. P. Shanley and K. Kurabayashi, *ACS Nano*, 2015, **9**(4), 4173–4181.



- 6 S. Zhang (Weihua) and W. Jian, *Rev. Anal. Chem.*, 2014, **33**(1), 31–47.
- 7 C. Dass, G. H. Fridland, P. W. Tinsley, J. T. Killmar and D. M. Desiderio, *Int. J. Pept. Protein Res.*, 1989, **34**(2), 81–87.
- 8 J. R. Barr, V. L. Maggio, D. G. Patterson, G. R. Cooper, L. O. Henderson, W. E. Turner, S. J. Smith, W. H. Hannon, L. L. Needham and E. J. Sampson, *Clin. Chem.*, 1996, **42**(10), 1676–1682.
- 9 E. Ciccimaro and I. A. Blair, *Bioanalysis*, 2010, **2**(2), 311–341.
- 10 J.-L. Hsu, S.-Y. Huang, N.-H. Chow and S.-H. C. Chen, *Anal. Chem.*, 2003, **75**(24), 6843–6852.
- 11 A. C. Tolonen and W. Haas, *JoVE*, 2014, **89**, 51416.
- 12 P. J. Boersema, R. Raijmakers, S. Lemeer, S. Mohammed and A. J. R. Heck, *Nat. Protoc.*, 2009, **4**(4), 484–494.
- 13 A. C. Tolonen, W. Haas, A. C. Chilaka, J. Aach, S. P. Gygi and G. M. Church, *Mol. Syst. Biol.*, 2011, **7**(1), 461.
- 14 P. J. Boersema, T. T. Aye, T. A. B. van Veen, A. J. R. Heck and S. Mohammed, *Proteomics*, 2008, **8**(22), 4624–4632.
- 15 F. Pailleux and F. Beaudry, *Biomed. Chromatogr.*, 2012, **26**(8), 881–891.
- 16 A. C. Peterson, J. D. Russell, D. J. Bailey, M. S. Westphall and J. J. Coon, *Mol. Cell. Proteomics*, 2012, **11**(11), 1475–1488.
- 17 N. Rauniyar, *Int. J. Mol. Sci.*, 2015, **16**(12), 28566–28581.
- 18 G. E. Ronsein, N. Pamir, P. D. von Haller, D. S. Kim, M. N. Oda, G. P. Jarvik, T. Vaisar and J. W. Heinecke, *J. Proteomics*, 2015, **113**, 388–399.
- 19 E. Kashuba, J. Bailey, D. Allsup and L. Cawkwell, *Biomarkers*, 2013, **18**(4), 279–296.
- 20 F. S. de Miranda, J. P. T. Guimarães, K. R. Menikdiwela, B. Mabry, R. Dhakal, R. I. Rahman, H. Moussa and N. Moustaid-Moussa, *Mol. Cell. Endocrinol.*, 2021, **528**, 111245.
- 21 H. Jia, *Shock*, 2016, **46**(3), 239–248.
- 22 K. Deepak, P. K. Roy, P. Kola, B. Mukherjee and M. Mandal, *Biochim. Biophys. Acta, Rev. Cancer*, 2022, **1877**(6), 188807.
- 23 M. Pahlavani, N. S. Kalupahana, L. Ramalingam and N. Moustaid-Moussa, in *Comprehensive Physiology*, ed. R. Terjung, Wiley, 2017, pp. 1137–1150.
- 24 Physiology, Renin Angiotensin System - StatPearls - NCBI Bookshelf.Html. <https://www.ncbi.nlm.nih.gov/pubmed/29261862>, last accessed 9 June 2023.
- 25 S. L. Cooper, E. Boyle, S. R. Jefferson, C. R. A. Heslop, P. Mohan, G. G. J. Mohanraj, H. A. Sidow, R. C. P. Tan, S. J. Hill and J. Woolard, *Int. J. Mol. Sci.*, 2021, **22**(15), 8255.
- 26 U.S. Food and Drug Administration, *Bioanalytical Method Validation. Guidance for Industry*, 2018, <https://www.fda.gov/files/drugs/published/Bioanalytical-Method-Validation-Guidance-for-Industry.pdf>.
- 27 T. Gangnus and B. B. Burckhardt, *Sci. Rep.*, 2021, **11**(1), 3061.
- 28 I. van den Broek, R. W. Sparidans, J. H. M. Schellens and J. H. Beijnen, *J. Chromatogr. B: Anal. Technol. Biomed. Life Sci.*, 2010, **878**(5–6), 590–602.
- 29 R. Liao, Y. Gao, M. Chen, L. Li and X. Hu, *Anal. Chem.*, 2018, **90**(22), 13533–13540.
- 30 R. Zhang, C. S. Sioma, R. A. Thompson, L. Xiong and F. E. Regnier, *Anal. Chem.*, 2002, **74**(15), 3662–3669.
- 31 E. Baralla, M. Nieddu, G. Boatto, M. V. Varoni, D. Palomba, M. P. Demontis, V. Pasciu and V. Anania, *J. Pharm. Biomed. Anal.*, 2011, **54**(3), 557–561.
- 32 A. Kutz, A. Conen, C. Gregoriano, S. Haubitz, D. Koch, O. Domenig, L. Bernasconi, B. Mueller and P. Schuetz, *Eur. J. Endocrinol.*, 2021, **184**(4), 543–552.
- 33 M. Rieder, L. Wirth, L. Pollmeier, M. Jeserich, I. Goller, N. Baldus, B. Schmid, H.-J. Busch, M. Hofmann, W. Kern, C. Bode, D. Duerschmied and A. Lothar, *Am. J. Hypertens.*, 2021, **34**(3), 278–281.
- 34 U. Kintscher, A. Slagman, O. Domenig, R. Röhle, F. Konietzschke, M. Poglitsch and M. Möckel, *Hypertension*, 2020, **76**(5), e34–e36.
- 35 A. L. V. Martins, F. A. da Silva, L. Bolais-Ramos, G. C. de Oliveira, R. C. Ribeiro, D. A. A. Pereira, F. Annoni, M. M. L. Diniz, T. G. F. Silva, B. Zivianni, A. C. Cardoso, J. C. Martins, D. Motta-Santos, M. J. Campagnole-Santos, F. S. Taccone, T. Verano-Braga and R. A. S. Santos, *ERJ Open Res.*, 2021, **7**, 00114–2021.
- 36 D. C. Files, K. W. Gibbs, C. L. Schaich, S. P. Collins, T. M. Gwathmey, J. D. Casey, W. H. Self and M. C. Chappell, *Am. J. Physiol.: Lung Cell. Mol. Physiol.*, 2021, **321**(1), L213–L218.
- 37 D. van Lier, M. Kox, K. Santos, H. van der Hoeven, J. Pillay and P. Pickkers, *ERJ Open Res.*, 2021, **7**(1), 00848–02020.
- 38 M. R. Garvin, C. Alvarez, J. I. Miller, E. T. Prates, A. M. Walker, B. K. Amos, A. E. Mast, A. Justice, B. Aronow and D. A. Jacobson, *eLife*, 2020, **9**, e59177.
- 39 D. A. B. Rex, N. Vaid, K. Deepak, S. Dagamajalu and T. S. K. Prasad, *Mol. Biol. Rep.*, 2022, **49**(10), 9915–9927.
- 40 E. Kashuba, J. Bailey, D. Allsup and L. Cawkwell, *Biomarkers*, 2013, **18**(4), 279–296.
- 41 G. M. d. M. Mendes, I. J. B. Do Nascimento, P. H. S. Marazzi-Diniz, I. B. Da Silveira, M. F. Itaborahy, L. E. Viana, F. A. Silva, M. F. Santana, R. A. A. Pinto, B. G. Dutra, M. V. G. Lacerda, S. A. Araujo, D. Wanderley, P. V. T. Vidigal, P. H. Diniz, T. Verano-Braga, R. A. S. Santos and M. F. Leite, *Front. Physiol.*, 2022, **13**, 1080837.
- 42 C. P. Martens, P. Van Mol, J. Wauters, E. Wauters, T. Gangnus, B. Noppen, H. Callewaert, J. H. M. Feyen, L. Liesenborghs, E. Heylen, S. Jansen, L. C. V. Pereira, S. Kraiss, I. Guler, M. M. Engelen, A. Ockerman, A. Van Herck, R. Vos, C. Vandenbriele, P. Meersseman, G. Hermans, A. Wilmer, K. Martinod, B. B. Burckhardt, M. Vanhove, M. Jacquemin, P. Verhamme, J. Neyts and T. Vanassche, *eBioMedicine*, 2022, **83**, 104195.
- 43 E. Alfaro, E. Díaz-García, S. García-Tovar, E. Zamarrón, A. Mangas, R. Galera, K. Nanwani-Nanwani, R. Pérez-de-Diego, E. López-Collazo, F. García-Río and C. Cubillos-Zapata, *Front. Immunol.*, 2022, **13**, 909342.

